Article:
Tickner, Benjamin, Svensson, S Karl-Mikael, Vaara, Juha et al. (1 more author) (2022) Towards Optimising and Understanding Reversible Hyperpolarisation of Lactate Esters Relayed from Parahydrogen. JOURNAL OF PHYSICAL CHEMISTRY LETTERS. 6859–6866. ISSN 1948-7185

https://doi.org/10.1021/acs.jpclett.2c01442

THE JOURNAL OF PHYSICAL CHEMISTRY LETTERS
A JOURNAL OF THE AMERICAN CHEMICAL SOCIETY

pubs.acs.org/JPCL

Letter

Toward Optimizing and Understanding Reversible Hyperpolarization of Lactate Esters Relayed from *para*-Hydrogen

Ben J. Tickner,* S. Karl-Mikael Svensson,* Juha Vaara,* and Simon B. Duckett*

Cite This: *J. Phys. Chem. Lett.* 2022, 13, 6859−6866

Read Online

ACCESS | Metrics & More | Article Recommendations | Supporting Information

ABSTRACT: The SABRE-Relay hyperpolarization method is used to enhance the ^{1}H and ^{13}C NMR signals of lactate esters, which find use in a wide range of medical, pharmaceutical, and food science applications. This is achieved by the indirect relay of magnetization from *para*-hydrogen, a spin isomer of dihydrogen, to OH-containing lactate esters via a SABRE-hyperpolarized NH intermediary. This delivers ^{1}H and ^{13}C NMR signal enhancements as high as 245- and 985-fold, respectively, which makes the lactate esters far more detectable using NMR. DFT-calculated *J*-couplings and spin dynamics simulations indicate that, while polarization can be transferred from the lactate OH to other ^{1}H nuclei via the *J*-coupling network, incoherent mechanisms are needed to polarize the ^{13}C nuclei at the 6.5 mT transfer field used. The resulting sensitivity boost is predicted to be of great benefit for the NMR detection and quantification of low concentrations (<mM) of lactate esters and could provide a useful precursor for the production of hyperpolarized lactate, a key metabolite.

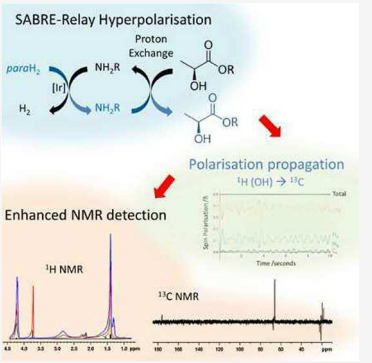

Lactate and lactate esters have many uses in medicine, biochemistry, and food science.[1−3] Detection of these molecules is vital for many applications from food quality control to early diagnosis and treatment of diseases such as cancer.[4−8] Nuclear magnetic resonance (NMR) is often the method-of-choice for molecular analysis as it allows direct detection of a molecule without sample destruction. However, NMR suffers from a high detection limit, which is usually compensated by signal averaging or using highly concentrated molecules (millimolar to molar) to generate sufficient signals. Many approaches have been developed to improve the sensitivity of NMR: perhaps the most successful is the advent of hyperpolarization.[9] Such techniques create molecules where the normal Boltzmann spin state population distribution is tipped to create a transient spin state that can be detected more easily.

In this work, we focus on hyperpolarization involving *para*-hydrogen (pH_2), a spin isomer of dihydrogen, as it is a versatile platform for the hyperpolarization of many biologically relevant disease markers.[5,10−13] Specifically, the signal amplification by reversible exchange (SABRE) method is employed here to enhance the NMR signals of lactate esters. SABRE utilizes the oxidative addition of pH_2 to form a hyperpolarized iridium dihydride complex (Figure 1a). Magnetization can then be transferred to other ligands within the complex in a process that is either spontaneous at low magnetic fields (mT[14] and μT[15]) or radiofrequency-driven at high field (T).[16] Spontaneous transfer at high fields (T) is also possible,[16−19] but ∼6.5 mT fields are typically employed for most efficient polarization transfer to the ^{1}H sites.[14,20] Under such conditions, polarization transfer occurs through the temporary *J*-coupled network formed within the transient organometallic complex[21] and level anticrossing descriptions are used to rationalize these effects.[22,23] Subsequently, dissociation of ligands from the polarization transfer catalyst gives rise to hyperpolarized molecules free in solution. Therefore, SABRE catalytically creates hyperpolarized target molecules continually and allows them to regenerate easily after they relax back to the non-hyperpolarized form. These considerations provide advantages when compared to other hyperpolarization techniques that are one-shot in nature. Furthermore, SABRE does not require target molecules to contain pH_2 acceptors or specialist equipment as its pH_2 feedstock is cheap and easy to produce.[24]

Currently, SABRE hyperpolarization is typically applied to substrates containing N-donor atoms, such as N-heterocycles,[14,20,25−27] amines,[28] and nitriles[29,30] although S-donor and O-donor targets, such as S-heterocycles[31] and ketoacids,[32,33] have also been hyperpolarized. Recently, relayed proton exchange effects (such as SABRE-Relay)[34] have expanded the substrate scope even further. In SABRE-Relay, a hyperpolarization carrier is used to transfer enhanced magnetization to a target molecule by proton exchange (Figure 1b). Amines or ammonia are typically used as hyperpolarization carriers as they have the N-donor motif required to form active $[Ir(H)_2(NHC)(NH_2R)_3]Cl$ catalysts necessary for the hyperpolarization of an amine or ammonia.[28,34,35] Exchange between carrier NH and OH protons in molecules, such as alcohols,[36] sugars,[37] silanols,[38] and many others[34,39]

Received: May 12, 2022
Accepted: June 21, 2022

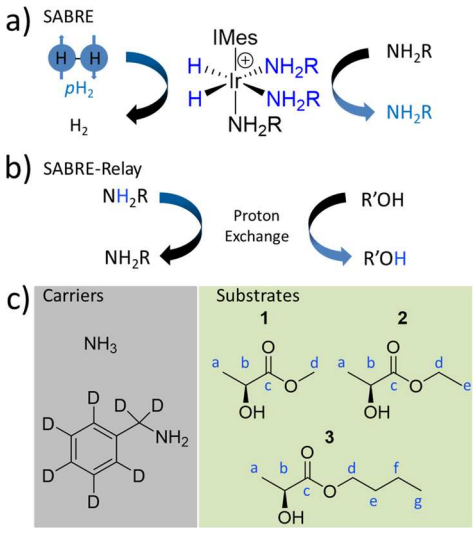

Figure 1. Summary of the SABRE and SABRE-Relay hyperpolarization methods and the substrates used in this work. (a) SABRE hyperpolarizes molecules without chemical alteration if the target molecule (here, NH_2R) and pH_2 are in reversible exchange at a polarization transfer catalyst. (b) The variant, SABRE-Relay exploits relayed proton exchange from a hyperpolarized source to enhance NMR signals in a target that is unable to coordinate to a SABRE catalyst. (c) The hyperpolarization carriers and hyperpolarization targets used in this work.

allows them to become hyperpolarized even though they do not have the typical iridium-ligating motifs required for direct SABRE. Most examples of molecules hyperpolarized using SABRE-Relay are simple OH-containing structures, with sugars representing perhaps the most complex targets hyperpolarized to date. So far, SABRE-Relay has achieved 2.6% ^{1}H,[36] 2.3% ^{29}Si,[38] 1.1% ^{13}C,[36,37] 0.2% ^{19}F,[36] and 0.04% ^{31}P[36] polarization levels. In this work, we aim to expand SABRE-Relay to hyperpolarize molecules of greater biological relevance such as the OH-containing lactate esters methyl lactate (**1**), ethyl lactate (**2**), and butyl lactate (**3**) (Figure 1c). Key factors that determine the efficiency of SABRE-Relay and how polarization spreads from the exchanging OH group to ^{1}H and ^{13}C sites within the target substrates are explored. We predict that this sensitivity boost will be of great use for the rapid NMR detection of lactate esters and could have implications for mixture analysis and disease diagnosis in the future.

This work begins with the formation of $[Ir(H)_2(IMes)(NH_3)_3]Cl$ and $[Ir(H)_2(IMes)(NH_2Bn\text{-}d_7)_3]Cl$ catalysts (where IMes is 1,3-bis(2,4,6-trimethyl-phenyl)imidazole-2-ylidene) by reaction of [IrCl(COD)(IMes)] (5 mM) (where COD is *cis,cis*-1,5-cyclooctadiene) with NH_3 (8−12 equiv) or $BnNH_2\text{-}d_7$ (5 equiv), respectively, alongside H_2 (3 bar) in dichloromethane-d_2 (0.6 mL) at room temperature overnight. NH_3 and $BnNH_2\text{-}d_7$ were selected as hyperpolarization carriers as they have been reported to yield the highest SABRE-Relay hyperpolarization levels in simple alcohols based on studies on a range of 24 different NH_2R carriers.[36] The formation of these polarization transfer catalysts is confirmed by the observation of characteristic ^{1}H NMR resonances.[28,34] At this point, **1**, **2**, or **3** (5 equiv) were added to the resulting solutions, under an N_2 atmosphere, before pH_2 (3 bar) was introduced. The NMR tube was then shaken manually for 10 s in the stray field of a 9.4 T spectrometer where the field was ∼6.5 mT. The metal: carrier and carrier: substrate ratios were fixed at 1:5−10 and 1:1, respectively, as these conditions have been reported to give the optimum relayed hyperpolarization levels in related substrates.[36,37] After shaking, the samples are rapidly inserted into the 9.4 T spectrometer for the collection of a single-scan hyperpolarized ^{1}H or ^{13}C NMR spectrum.

When such SABRE-Relay experiments are performed, enhanced ^{1}H NMR signals for **1**, **2**, or **3** can be observed (Figure 2a and b). These enhanced signals are broadened relative to their thermally polarized counterparts and this is likely related to sample movement and nonoptimal shimming using this manual sample shaking and insertion method. The use of automated systems could reflect a route to reduce line broadness.[40,41] The highest ^{1}H NMR signal enhancements were seen for the CH group or lactate CH_3 group, with polarization transfer across the ester group into the methyl, ethyl, or butyl groups in **1**, **2**, or **3**, respectively, being less significant (Table 1). Prior relaxation of the associated nonequilibrium population differences will play an important role in determining these measured NMR signal enhancements and therefore the relaxation times of the ^{1}H resonances of **1**−**3** in these mixtures were determined (Table 1). It might be expected that the aliphatic sites with the highest NMR signal enhancements are associated with long T_1 values. This is true for **1** in which the CH site with the longest T_1 time (29.3 s) has the highest ^{1}H NMR signal enhancement (55-fold). However, these trends are not always consistent as the lactate CH_3 group within **1** contains the shortest T_1 within the molecule (5.9 s) and yet exhibits a modest 30-fold ^{1}H NMR signal enhancement. In other words, the low ^{1}H NMR signal enhancements of sites in the ester chains of **1**−**3** are not necessarily just associated with rapid proton relaxation (Table 1). When these experiments were repeated using the $BnNH_2\text{-}d_7$ carrier, the trends in ^{1}H NMR signal enhancement proved similar, with the polarization gain remaining predominantly localized on the lactate CH and CH_3 groups. For the ^{1}H NMR signal enhancements of these substrates, $BnNH_2\text{-}d_7$ proves to be more efficient than NH_3 as it gives rise to higher enhancements for every site of **1** and **2** when compared to those with NH_3, whereas the ^{1}H NMR signal enhancements of **3** are comparable for both carriers. Previous investigations have suggested that when NH_3 and $BnNH_2\text{-}d_7$ are compared as SABRE targets, greater NH polarization results for $BnNH_2\text{-}d_7$.[28,36] We, therefore, link the amount of substrate OH polarization to the finite polarization of the carrier NH available for relay into the lactate esters after exchange. It generally appears that the average ^{1}H NMR signal enhancements per site decrease as the length of the ester chain increases in accordance with the fact that the finite OH polarization is shared among more protons. Greater distances between the exchanging OH group and remote aliphatic sites in the ester side arm are also likely to play a role in reducing the efficiency of polarization transfer to distant sites.[12,42,43]

When similar single-scan hyperpolarized ^{13}C NMR measurements are recorded on the samples of **1**−**3** with NH_3 or $BnNH_2\text{-}d_7$, carriers, enhanced ^{13}C NMR signals can also be detected despite the fact that the lactate esters are in a non-^{13}C-labeled form (Figure 2c and d, Table 1). Significant ^{13}C NMR signal enhancements are seen for the lactate CH and CH_3 (>95-fold) groups with smaller values achieved for the ester carbonyl (<85-fold). The site with the highest ^{13}C NMR signal gain is now dependent on the substrate and carrier. For **1**, the lactate CH_3 site was enhanced to greater extent than the CH site when NH_3 was used as a carrier (625- versus 595-fold,

https://doi.org/10.1021/acs.jpclett.2c01442
J. Phys. Chem. Lett. 2022, 13, 6859−6866

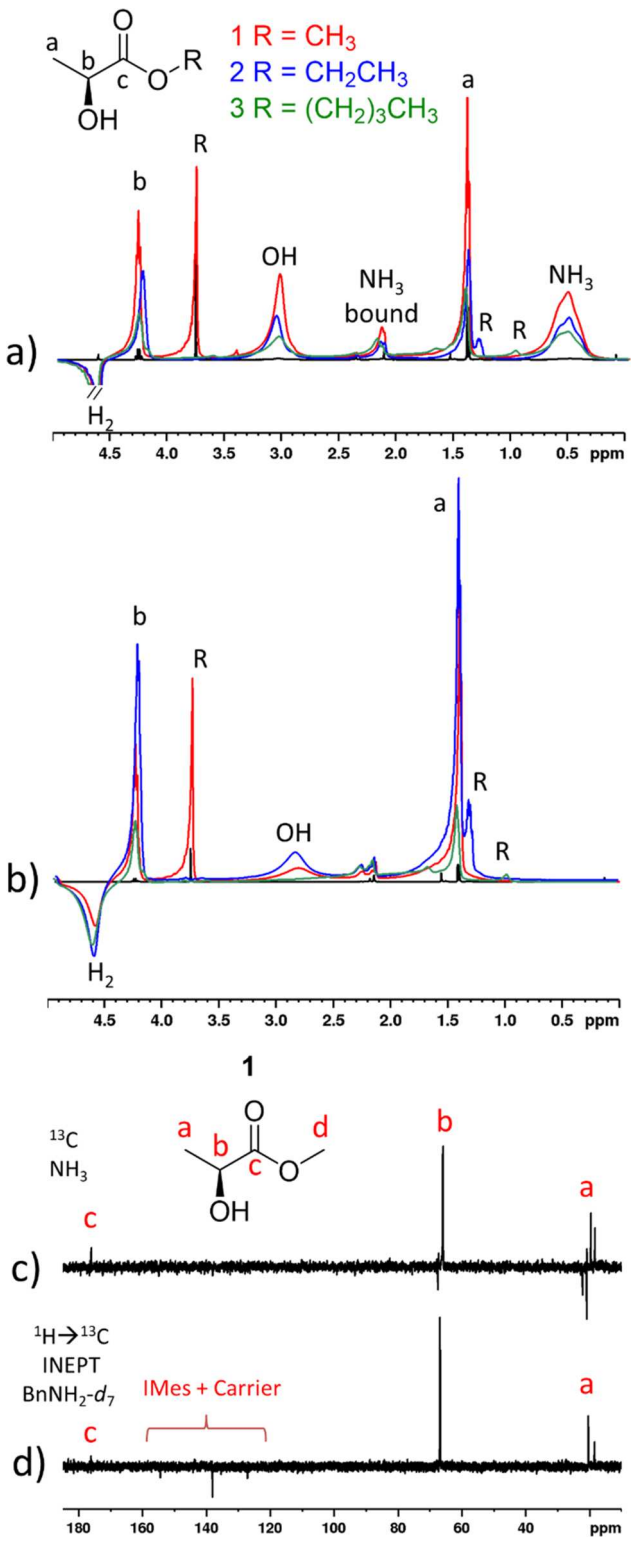

Figure 2. Hyperpolarized NMR spectra. Selected regions of single-scan (a, b) ^{1}H, (c) ^{13}C, and (d) ^{1}H decoupled ^{13}C INEPT (short-range) NMR spectra recorded at 9.4 T and 298 K after samples containing (a, c) NH_3 (8−12 equiv) or (b, d) $BnNH_2$-d_7 (5 equiv) with [IrCl(COD)(IMes)] (5 mM) and the indicated lactate ester in 0.6 mL of dichloromethane-d_2 are shaken with 3-bar pH_2 for 10 s at 6.5 mT. In panels a and b, the corresponding single-scan thermally polarized spectrum for **1** is shown in black for comparison. More detailed NMR spectra are provided in the Supporting Information, section S2. Thermally polarized ^{13}C and INEPT NMR spectra are provided in the Supporting Information, section S3, for comparison.

respectively), although when $BnNH_2$-d_7 was employed the CH polarization was greater (310- versus 335-fold, respectively). However, for **3**, the CH site received the greatest share of polarization (165- versus 255-fold with NH_3 and $BnNH_2$-d_7 carriers, respectively, compared to CH_3 gains of 195- and 150-fold, respectively). For **2**, NH_3 again delivered the highest ^{13}C polarization on the lactate CH_3 site when compared to the CH site (640- versus 420-fold) but $BnNH_2$-d_7 enhances the CH signal more than the CH_3 (345- versus 270-fold). This behavior suggests that the OH/NH exchange rate, which will differ for the two carriers, must influence the degree of polarization transfer from OH into the ^{13}C nuclei. Visible OH polarization is clearly higher using $BnNH_2$-d_7 when compared to NH_3, which is reflected in generally better ^{1}H performance but worse ^{13}C gains. Exchange of the OH group proton will destroy the *J*-coupling network that is associated with propagation of polarization. Therefore, the residence time of the enhanced OH proton is concluded to be extremely important.[44] This fact highlights the tension between initial carrier polarization, efficiency of the relayed NH/OH exchange, and subsequent propagation of OH polarization to other ^{1}H and ^{13}C sites within the substrate. At the 65 G polarization transfer fields in these experiments, ^{13}C polarization was localized exclusively within the lactate unit and did not spread across the carbonyl group to the ester chains of the substrates. It is worth noting that transfer to distant ^{13}C sites may be possible using field cycling regimes at low magnetic fields (i.e., μT): such effects have been demonstrated for related molecules.[5,12,42] For utilization of these enhanced ^{13}C MR signals, it is important that hyperpolarization resides most predominantly on sites with the longest relaxation time as this allows the hyperpolarized state to be detected over much longer time windows which is useful for reaction monitoring[45,46] or biomedical imaging applications.[47] Estimates of hyperpolarized ^{13}C magnetization lifetimes of **1**−**3** were measured at 9.4 T by leaving the hyperpolarized sample (with carrier and catalyst) in the magnet for a varying time interval before recording a single-scan ^{13}C NMR spectrum. This yielded T_1 values of ∼<5, ∼20, and ∼50 s for the CH_3, CH, and CO sites, respectively (see Figure S17). These compare well with values reported in the literature for lactate and similar molecules and confirm that the carbonyl carbon, which is more isolated from the other NMR-active spins within the molecule, has the longest T_1.[5,6,48] Unfortunately, in our SABRE-Relay experiments on **1**−**3** discussed so far the majority of the attained ^{13}C polarization resides on the more rapidly relaxing CH_3 and CH groups and only modest (<100-fold) signal enhancements can be achieved for the slowly relaxing CO site.

To enhance the degree of magnetization transfer to the carbonyl site, ^{1}H → ^{13}C INEPT (insensitive nuclei enhanced by polarization transfer) pulse sequences were used to transfer the SABRE-Relay derived ^{1}H polarization to ^{13}C sites in the molecule. These sequences contain a variable time delay that is related to the size of the *J*-coupling connecting the ^{1}H−^{13}C spin pair between which magnetization is transferred. NMR pulse sequences were used with two sets of arbitrary time delays corresponding to polarization transfer between ^{1}H−^{13}C spin pairs with 125 Hz (short-range) and 10 Hz (long-range) coupling (see Supporting Information, section S1.2). The effect of these ^{1}H → ^{13}C INEPT sequences, following the hyperpolarization process of **1**−**3** using SABRE-Relay, was examined by calculating the ^{13}C NMR signal enhancements by

https://doi.org/10.1021/acs.jpclett.2c01442
J. Phys. Chem. Lett. 2022, 13, 6859−6866

Table 1. Summary of SABRE-Relay NMR Signal Enhancements[a]

		^{1}H NMR signal enhancement (fold)		^{1}H T_1 (s)	^{13}C NMR signal enhancement (fold)					
					^{13}C NMR		^{1}H and ^{13}C INEPT short-range		^{1}H and ^{13}C INEPT long-range	
substrate	site	carrier NH_3	carrier $BnNH_2$-d_7	carrier NH_3	carrier NH_3	carrier $BnNH_2$-d_7	carrier NH_3	carrier $BnNH_2$-d_7	carrier NH_3	carrier $BnNH_2$-d_7
1	a	30 ± 5	110 ± 10	5.9	625 ± 5	310 ± 40	175 ± 10	55 ± 5	30 ± 5	15 ± 5
	b	55 ± 5	115 ± 10	29.3	595 ± 30	335 ± 25	400 ± 55	150 ± 5	390 ± 50	70 ± 5
	c	N/A	N/A	N/A	85 ± 10	35 ± 5	0	305 ± 20	70 ± 15	30 ± 5
	d	15 ± 5	40 ± 5	10.9	0	0	0	0	0	0
	OH	80 ± 5	310 ± 10	5.8	N/A	N/A	N/A	N/A	N/A	N/A
	average	35 ± 5	85 ± 5	N/A	375 ± 10	195 ± 20	320 ± 40	115 ± 5	145 ± 20	35 ± 5
	NH (free)	70 ± 5	N/A	6.2	N/A	N/A	N/A	N/A	N/A	N/A
2	a	15 ± 5	135 ± 5	5.0	640 ± 5	270 ± 5	55 ± 5	55 ± 5	15 ± 5	20 ± 5
	b	15 ± 5[b]	90 ± 5[b]	12.0[b]	420 ± 45	345 ± 20	115 ± 15	185 ± 10	130 ± 40	120 ± 10
	c	N/A	N/A	N/A	85 ± 10	50 ± 5	0	335 ± 50	100 ± 30	120 ± 5
	d	15 ± 5[b]	90 ± 5[b]	12.0[b]	0	0	0	0	0	0
	e	2 ± 1	20 ± 5	8.1	0	0	0	0	0	0
	OH	40 ± 10	165 ± 5	4.8	N/A	N/A	N/A	N/A	N/A	N/A
	average	15 ± 5	80 ± 5	N/A	390 ± 20	140 ± 5	125 ± 20	140 ± 5	85 ± 20	70 ± 5
	NH (free)	30 ± 5	N/A	4.4	N/A	N/A	N/A	N/A	N/A	N/A
3	a	20 ± 5[b]	20 ± 5[b]	4.0[£]	120 ± 25	95 ± 5	30 ± 5	60 ± 5	0	20 ± 5
	b	40 ± 5[+]	70 ± 5[+]	12.8[+]	165 ± 35	255 ± 15	110 ± 10	5 ± 1	45 ± 15	80 ± 15
	c	N/A	N/A	N/A	35 ± 5	40 ± 5	0	3 ± 1	75 ± 5	35 ± 5
	d	10 ± 5[+]	10 ± 5[+]	5.6[+]	0	0	0	0	0	0
	e	25 ± 5	25 ± 5	5.1	0	0	0	0	0	0
	f	20 ± 5[b]	20 ± 5[b]	5.4[£]	0	0	0	0	0	0
	g	7 ± 1	5 ± 1	5.7	0	0	0	0	0	0
	OH	50 ± 5	N/A	4.7	N/A	N/A	N/A	N/A	N/A	N/A
	average	20 ± 5	20 ± 5	N/A	110 ± 20	130 ± 5	95 ± 10	15 ± 5	40 ± 5	15 ± 5
	NH (free)	75 ± 10	N/A	5.8	N/A	N/A	N/A	N/A	N/A	N/A

[a]^{1}H and ^{13}C NMR signal enhancements (per site) for **1**−**3** when each (5 equiv) is shaken with 3-bar pH_2 for 10 s at 6.5 mT in an activated solution of [IrCl(COD)(IMes)] (5 mM) with NH_3 (8−12 equiv) or $BnNH_2$-d_7 (5 equiv) in dichloromethane-d_2 (0.6 mL). The sites are labelled according to Figure 1c. ^{1}H T_1 values were measured at 9.4 T using inversion recovery. Note that the average polarization refers to the total hyperpolarized integral intensity of the substrate divided by its thermally polarized counterpart and reflects an average substrate polarization per ^{1}H or ^{13}C site. NH (free) refers to the polarization (per site) for the carrier NH. [b]Values are averaged across the two sites due to signal overlap; [+,£]Signals overlap.

reference to thermally polarized ^{1}H → ^{13}C INEPT sequences recorded using the same delay times and acquisition parameters (Table 1). ^{13}C NMR signal enhancements for the lactate CH and CH_3 sites within **1**−**3** were higher using direct ^{13}C NMR detection as compared to the ^{1}H → ^{13}C INEPT detection, regardless of the carrier or INEPT sequence used (Table 1). Optimized INEPT sequences can theoretically boost ^{13}C polarization by a factor of 4, which reflects the four times larger gyromagnetic ratio of ^{1}H nuclei. The INEPT ^{13}C NMR signal enhancements recorded here do not achieve this level of ^{13}C sensitivity boost (Table 1). We expect factors, such as OH exchange and relaxation, during the mixing time of these INEPT experiments to decrease their efficiency, effects that become more evident for "short-range" INEPT sequences containing longer time delays. In our experiments, it is challenging to attribute a combined ^{13}C NMR signal enhancement factor resulting from combined SABRE-Relay and INEPT methods due to differing acquisition parameters. Nevertheless, we suggest that true hyperpolarized ^{13}C INEPT NMR signal enhancements compared to thermally polarized direct ^{13}C NMR detection are ∼1−2 times larger than the signal enhancements presented in Table 1, which quotes values relative to thermally polarized ^{1}H → ^{13}C INEPT control measurements. There is, however, a significant uplift in the CO polarization level of the longer-lived carbonyl sites. For instance, 305- and 335-fold ^{13}C NMR signal enhancements could be achieved for **1** and **2** respectively using the $BnNH_2$-d_7 carrier and short-range ^{1}H → ^{13}C INEPT sequences, which is higher than the 35-fold and 50-fold achieved for the same samples with standard ^{13}C NMR detection. Interestingly, this increase in carbonyl site ^{13}C polarization using the short-range INEPT sequence suggests that polarization transfer from OH to CO sites is now efficient even though the J coupling is mismatched. There is, however, a dramatic difference between differing carriers, which suggests that the OH/NH exchange has a major impact. For example, in samples involving NH_3 as a carrier, ^{13}C NMR signal enhancements for the carbonyl site of **2** and **3** detected using INEPT sequences optimized for long-range ^{1}H−^{13}C couplings (10 Hz) were higher when compared to direct ^{13}C NMR detection. However, for samples containing $BnNH_2$-d_7, use of short-range (125 Hz) ^{1}H → ^{13}C INEPT sequences yielded much better ^{13}C NMR carbonyl signal enhancement in **1**−**3** when compared to direct ^{13}C NMR detection. These results highlight that there is no one set of standard conditions that deliver optimal SABRE-Relay NMR signal enhancements in all three substrates and suggest that further development and the use of novel sequences[49−52] with optimized delay times may constitute a valuable route to increase these ^{13}C signal gains further.

https://doi.org/10.1021/acs.jpclett.2c01442
J. Phys. Chem. Lett. 2022, 13, 6859−6866

The initial SABRE effect, in which spin order is transferred from pH_2-derived hydride ligands to the NH site of a bound carrier molecule, is driven by formation of a transient *J*-coupled network.[21,22,53] Upon NH/OH exchange, polarization propagation to other ^{1}H and ^{13}C sites within the lactate ester could occur through *J*-coupling in a similar fashion. To gain a greater understanding of these effects, density functional theory (DFT) calculations were performed to predict the *J*-couplings within **1**-**3** that are involved in these polarization transfer processes (Supporting Information, Tables S5−7). Overall, the short-range computed coupling constants are in fairly good agreement with values obtained from experiment (Supporting Information, Tables S5−7). Furthermore, these calculations determine long-range *J*-coupling values that we could not discern from ^{1}H or ^{13}C NMR spectra and could play an important role in polarization propagation. The results show that the *J* coupling between the OH proton and the carbonyl carbon is just 5−6 Hz. Small *J*-couplings will also play a role if polarization transfer from OH is indirectly propagated to the carbonyl carbon according to a OH → H_b → C_c pathway, with the latter step no longer being inhibited by OH exchange. Computationally, the OH → H_b → C_c transfer pathway involves small *J* couplings of <5 Hz. A route involving a larger 56−57 Hz coupling C_b → C_c could operate, but this will be limited by the natural ^{13}C abundance and a large J_{CC} splitting is not observed for the carbonyl signal in hyperpolarized spectra. Crucially, these *J*-couplings prove to be similar for **1**−**3**, which suggests that the differences in substrate ^{1}H and ^{13}C polarization levels that are observed are not due to significant differences in the spin coupling topology within these CH frameworks.

Spin dynamics simulations were performed to predict how coherent polarization transfer might occur via the *J*-coupling network from the OH spin to the other spins within the lactate ester framework. Different spin systems were simulated, taking into account the fact that natural abundance ^{13}C was involved in the experiments. Initially, a 5-spin model consisting of OH, H_b, and three H_a protons was used to study polarization transfer within the proton-only spin system. These simulations allow evolution of an initial 100% OH nuclear spin polarization during a 10-s shaking period at a given polarization transfer field (0 T, 6.5 mT, or 9.4 T) to the other ^{1}H spins. These simulations reflect an ideal experiment free from the effects of OH/NH exchange and T_1 relaxation. Simulations for this system show that spin polarization transfer occurs between all the included ^{1}H spins at the lower polarization transfer fields (0 T and 6.5 mT), but essentially no spin polarization transfer occurs at 9.4 T (see Supporting Information, Figures S19−S21). Furthermore, 6-spin systems involving one of the $^{13}C_a$, $^{13}C_b$, or $^{13}C_c$ centers were simulated to investigate polarization transfer to ^{13}C, as in most ^{13}C-containing molecules there is only one naturally abundant ^{13}C nucleus (see Figure 3 and Supporting Information, Figures S19−S21). Sites in the ester side chain were not included as ^{13}C NMR experiments do not exhibit enhanced magnetization for these sites at a 6.5 mT transfer field. For these 6-spin systems, simulations show that at polarization transfer fields of 0 and 9.4 T they behave similarly to the 5-spin ^{1}H systems, with spin polarization transfer to all spins at 0 T and not to any noticeable extent to any spin at 9.4 T. At a polarization transfer field of 6.5 mT, the simulations show that the presence of a ^{13}C (i.e., in about 1% of the molecules at natural abundance), reduces the spin polarization transfer between the protons by perturbing the spin−spin coupling network, without any noticeable spin polarization being transferred to the ^{13}C. Under such idealized conditions, the simulations reveal that coherent polarization transfer from OH to H_a and H_b can occur at 6.5 mT, but transfer to the ^{13}C subsystem does not. This suggests that other, incoherent routes, such as cross relaxation, have to dominate the OH → ^{13}C polarization propagation at the 6.5 mT polarization transfer fields necessary to achieve optimal ^{1}H polarization via SABRE-Relay. This finding supports previous theoretical studies.[44]

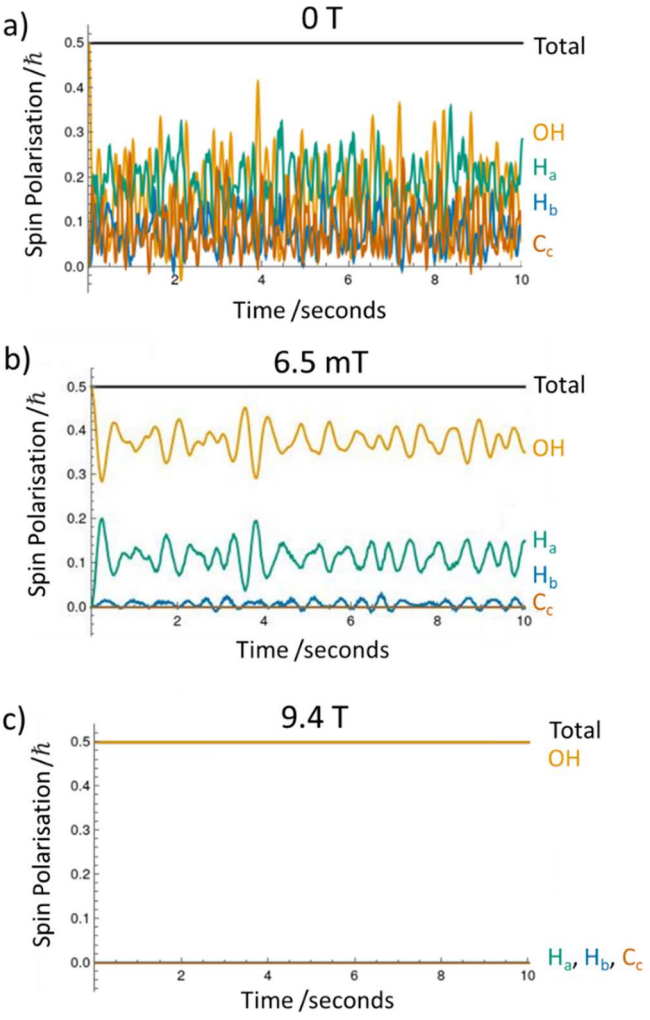

Figure 3. Simulating polarization propagation. Simulated spin polarization as a function of time for the different sites of a 6-spin system ($3H_a$, H_b, OH, and C_c) at (a) 0 T, (b) 6.5 mT, and (c) 9.4 T.

The results presented so far highlight that there is no one set of standard conditions that achieve optimal SABRE-Relay NMR signal enhancements for all substrates. Optimization of magnetization on a particular site, or particular nuclei (^{1}H or ^{13}C in this work), is likely to require a different set of conditions, even for optimization of NMR signal enhancements on different sites, or for different nuclei, in the same molecule using the same carrier. To highlight this point, SABRE-Relay hyperpolarization of **2** was tested with different amounts of the carrier NH_3. These results show that the ^{1}H NMR signal enhancements for the lactate CH_3, CH and OH sites could be dramatically increased from 15-, 15-, and 40-fold using 9 equiv NH_3 to 215-, 160-, and 245-fold, when the amount of NH_3 was lowered to 6.5 equiv (Figure 4a). Similar

https://doi.org/10.1021/acs.jpclett.2c01442
J. Phys. Chem. Lett. 2022, 13, 6859−6866

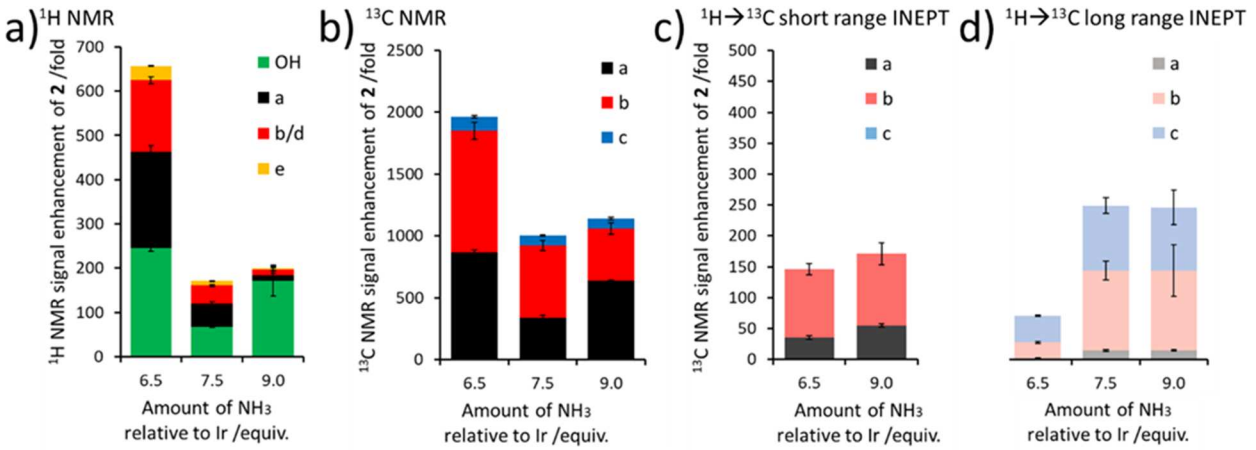

Figure 4. Toward optimizing SABRE-Relay. (a) ^{1}H and (b) ^{13}C NMR signal enhancements of **2** achieved using SABRE-Relay as a function of carrier NH_3 concentration. ^{13}C NMR signal enhancements achieved using (c) short-range and (d) long-range ^{1}H→ ^{13}C INEPT sequences are also shown. A full table of NMR signal enhancements is given in the Supporting Information, Table S9.

increases of ^{13}C NMR signal enhancements from 640-, 420, and 85-fold for the CH_3, CH, and CO sites, respectively, to 865-, 985- and 110-fold, respectively (Figure 4b), were observed. Interestingly, this same improvement in ^{13}C NMR signal enhancement at lower NH_3 concentration was not observed in the data collected by ^{1}H → ^{13}C INEPT transfer (Figure 4c and d). This suggests that a lower NH_3 amount corresponds to more optimal, likely slower, NH/OH exchange and benefits the direct ^{1}H and ^{13}C NMR detection.

The substrates **1**−**3** used in this work are liquids at room temperature and pressure. Hyperpolarization of protic molecules that are not soluble in nonprotic SABRE-Relay compatible solvents can be challenging because nonspecific proton exchange is undesirable. For example, attempts to hyperpolarize sodium lactate by SABRE-Relay fail due to the presence of water; 10 μL is required to solubilize it in CD_2Cl_2 or $CDCl_3$ solvents (see Supporting Information, section S10). Furthermore, doping SABRE-Relay samples of **1**−**3** with water leads to a drop in the delivered NMR signal enhancements (see Supporting Information, section S9). Similar effects have been reported for other substrates.[36,37] Hyperpolarization of **1**-**3** could therefore provide a route to hyperpolarize sodium lactate. To this end, SABRE-Relay could be used with rapid hydrolysis of the ester side chain to form lactate in an approach that is similar to PHIP-SAH which has already achieved significant lactate ^{13}C polarization.[5] In preliminary experiments we confirmed that hydrolysis and phase separation of **2** could indeed yield aqueous solutions of lactate (see Supporting Information, section S10). However, these steps took ∼90 s in our nonoptimized setup and, therefore, have not yet yielded enhanced NMR signals for lactate. In the future, optimization of ^{13}C NMR signal gains on the carbonyl site, followed by rapid hydrolysis, will likely open a route to produce hyperpolarized lactate. This approach could be extended to a wider range of molecules that contain the OH-groups necessary for SABRE-Relay but are not soluble in compatible solvents. They could be functionalized as esters with a side arm that alters solubility. This would allow them to be hyperpolarized using SABRE-Relay before the target molecule is released in a rapid hydrolysis step.

In conclusion, hyperpolarization of lactate esters using SABRE-Relay has been presented. ^{1}H and ^{13}C polarization is predominantly localized within the lactate CH and CH_3 groups with lower signal enhancements for the carbonyl carbon and little polarization transfer to the ester side arm. Optimization and rationalization of SABRE-Relay efficiency can be extremely challenging with many factors such as carrier NH polarization, OH/NH exchange efficiency, and polarization propagation from OH to other sites with the substrate all being important steps that can be influenced by the carrier, substrate, and their ratios. ^{1}H and ^{13}C NMR enhancements as high as 245-fold (0.8% polarization) and 985-fold (0.8% polarization), respectively, for lactate esters have been achieved using the SABRE-Relay approach. We have also demonstrated that ^{1}H → ^{13}C INEPT sequences can in some cases improve polarization of the longer-lived carbonyl site (up to 335-fold ^{13}C NMR enhancement using hyperpolarized INEPT). These sensitivity improvements have allowed the detection of 25 mM concentrations of lactate esters in just a single-scan ^{13}C NMR spectrum, which are not discerned using thermally polarized NMR. Examination of a wider range of INEPT sequences,[6,49,54,55] further optimization of sequence mixing times, or even magnetic field cycling approaches,[5,42] are likely to increase these NMR signal enhancements. Relayed substrate/carrier exchange influences polarization propagation within the substrate, despite theoretical calculations showing similar spin topologies within the substrates used here. Spin dynamics simulations indicate that polarization transfer from the OH proton to the other ^{1}H sites of the substrate readily takes place via the spin−spin coupling network at the polarization transfer field of 6.5 mT. In contrast, polarization of the ^{13}C spin subsystem is deduced to occur via incoherent mechanisms, at this polarization transfer field. It is likely that both *J*-coupling and cross-relaxation effects can play a role in polarization transfer to heteronuclei depending on the spin topology of the substrate and the polarization transfer field. In the future, further studies to understand and optimize relayed polarization transfer would be highly beneficial because of the wider range of molecules whose NMR signals could be enhanced by the technique.

■ ASSOCIATED CONTENT

Supporting Information

The Supporting Information is available free of charge at https://pubs.acs.org/doi/10.1021/acs.jpclett.2c01442.

https://doi.org/10.1021/acs.jpclett.2c01442
J. Phys. Chem. Lett. 2022, 13, 6859−6866

Experimental methods, computational details, additional NMR spectra (PDF)

Code for simulation of polarization transfer and NMR spectra (PDF, ZIP)

AUTHOR INFORMATION

Corresponding Authors

Ben J. Tickner − *Centre for Hyperpolarisation in Magnetic Resonance, Department of Chemistry, University of York, Heslington, United Kingdom YO10 5NY; NMR Research Unit, University of Oulu, FI-90014 Oulu, Finland;* orcid.org/0000-0002-8144-5655; Email: ben.tickner@alumni.york.ac.uk

S. Karl-Mikael Svensson − *NMR Research Unit, University of Oulu, FI-90014 Oulu, Finland;* orcid.org/0000-0002-7895-6876; Email: karl-mikael.svensson@oulu.fi

Juha Vaara − *NMR Research Unit, University of Oulu, FI-90014 Oulu, Finland;* orcid.org/0000-0002-1179-4905; Email: juha.vaara@oulu.fi

Simon B. Duckett − *Centre for Hyperpolarisation in Magnetic Resonance, Department of Chemistry, University of York, Heslington, United Kingdom YO10 5NY;* orcid.org/0000-0002-9788-6615; Email: simon.duckett@york.ac.uk

Complete contact information is available at: https://pubs.acs.org/10.1021/acs.jpclett.2c01442

Notes

The authors declare no competing financial interest.

Data can be found at https://pure.york.ac.uk/portal/en/.

ACKNOWLEDGMENTS

Dr. Victoria Annis is thanked for synthesis of the [IrCl(COD)(IMes)] precatalyst. Dr. Peter J. Rayner is thanked for helpful discussions. B.J.T. would like to thank the EPSRC for his studentship. S.K.-M.S. and J.V. acknowledge funding from the Academy of Finland (Grant 331008) and the University of Oulu (Kvantum Institute). Computations were carried out at CSC—the Finnish IT Center for Science and the Finnish Grid and Cloud Infrastructure project (persistent identifier urn:nbn:fi:research-infras-2016072533). S.B.D acknowledges the Wellcome Trust (Grants 092506 and 098335), the MRC (MR/M008991/1), and the University of York for financial support.

REFERENCES

(1) Abd Alsaheb, R. A.; Aladdin, A.; Othman, N. Z.; Abd Malek, R.; Leng, O. M.; Aziz, R.; el Enshasy, H. A. Lactic Acid Applications in Pharmaceutical and Cosmeceutical Industries. *J. Chem. Pharmaceutical Res.* **2015**, *7* (10), 729−735.

(2) Pereira, C. S. M.; Silva, V. M. T. M.; Rodrigues, A. E. Ethyl Lactate as a Solvent: Properties, Applications and Production Processes-a Review. *Green Chem.* **2011**, *13* (10), 2658−2671.

(3) Prottey, C.; George, D.; Leech, R. W.; Black, J. G.; Howes, D.; Vickers, C. F. H. The Mode of Action of Ethyl Lactate as a Treatment for Acne. *Br. J. Dermatol.* **1984**, *110* (4), 475−485.

(4) Pundir, C. S.; Narwal, V.; Batra, B. Determination of Lactic Acid with Special Emphasis on Biosensing Methods: A Review. *Biosens. Bioelec.* **2016**, *86*, 777−790.

(5) Cavallari, E.; Carrera, C.; Aime, S.; Reineri, F. 13C MR Hyperpolarization of Lactate by Using Parahydrogen and Metabolic Transformation in Vitro. *Chem. Eur. J.* **2017**, *23* (5), 1200−1204.

(6) Wang, J.; Kreis, F.; Wright, A. J.; Hesketh, R. L.; Levitt, M. H.; Brindle, K. M. Dynamic 1H Imaging of Hyperpolarized [1−13C] Lactate in Vivo Using a Reverse INEPT Experiment. *Magn. Reson. Med.* **2018**, *79* (2), 741−747.

(7) Chen, A. P.; Kurhanewicz, J.; Bok, R.; Xu, D.; Joun, D.; Zhang, V.; Nelson, S. J.; Hurd, R. E.; Vigneron, D. B. Feasibility of Using Hyperpolarized [1−13C] Lactate as a Substrate for in Vivo Metabolic 13C MRSI Studies. *Magn. Reson. Im.* **2008**, *26* (6), 721−726.

(8) Rattu, G.; Khansili, N.; Maurya, V. K.; Krishna, P. M. Lactate Detection Sensors for Food, Clinical and Biological Applications: A Review. *Environ. Chem. Lett.* **2021**, *19* (2), 1135−1152.

(9) Nikolaou, P.; Goodson, B. M.; Chekmenev, E. Y. NMR Hyperpolarization Techniques for Biomedicine. *Chem. Eur. J.* **2015**, *21* (8), 3156−3166.

(10) Ripka, B.; Eills, J.; Kouřilová, H.; Leutzsch, M.; Levitt, M. H.; Münnemann, K. Hyperpolarized Fumarate via Parahydrogen. *Chem. Commun.* **2018**, *54* (86), 12246−12249.

(11) Bhattacharya, P.; Chekmenev, E. Y.; Perman, W. H.; Harris, K. C.; Lin, A. P.; Norton, V. A.; Tan, C. T.; Ross, B. D.; Weitekamp, D. P. Towards Hyperpolarized 13C-Succinate Imaging of Brain Cancer. *J. Magn. Reson.* **2007**, *186* (1), 150−155.

(12) Reineri, F.; Boi, T.; Aime, S. Parahydrogen Induced Polarization of 13C Carboxylate Resonance in Acetate and Pyruvate. *Nat. Commun.* **2015**, *6*, 5858.

(13) Hövener, J.; Pravdivtsev, A. N.; Kidd, B.; Bowers, C. R.; Glöggler, S.; Kovtunov, K. V.; Plaumann, M.; Katz-Brull, R.; Buckenmaier, K.; Jerschow, A.; et al. Parahydrogen-based Hyperpolarization for Biomedicine. *Angew. Chem., Int. Ed.* **2018**, *57* (35), 11140−11162.

(14) Adams, R. W.; Aguilar, J. A.; Atkinson, K. D.; Cowley, M. J.; Elliott, P. I. P.; Duckett, S. B.; Green, G. G. R.; Khazal, I. G.; López-Serrano, J.; Williamson, D. C. Reversible Interactions with Para-Hydrogen Enhance NMR Sensitivity by Polarization Transfer. *Science* **2009**, *323* (5922), 1708−1711.

(15) Theis, T.; Truong, M. L.; Coffey, A. M.; Shchepin, R. V.; Waddell, K. W.; Shi, F.; Goodson, B. M.; Warren, W. S.; Chekmenev, E. Y. Microtesla SABRE Enables 10% Nitrogen-15 Nuclear Spin Polarization. *J. Am. Chem. Soc.* **2015**, *137* (4), 1404−1407.

(16) Barskiy, D. A.; Kovtunov, K. V.; Koptyug, I. V.; He, P.; Groome, K. A.; Best, Q. A.; Shi, F.; Goodson, B. M.; Shchepin, R. V.; Coffey, A. M.; et al. The Feasibility of Formation and Kinetics of NMR Signal Amplification by Reversible Exchange (SABRE) at High Magnetic Field (9.4 T). *J. Am. Chem. Soc.* **2014**, *136* (9), 3322−3325.

(17) Pravdivtsev, A. N.; Yurkovskaya, A. V.; Zimmermann, H.; Vieth, H.-M.; Ivanov, K. L. Enhancing NMR of Insensitive Nuclei by Transfer of SABRE Spin Hyperpolarization. *Chem. Phys. Lett.* **2016**, *661*, 77−82.

(18) Knecht, S.; Kiryutin, A. S.; Yurkovskaya, A. V.; Ivanov, K. L. Efficient Conversion of Anti-Phase Spin Order of Protons into 15N Magnetisation Using SLIC-SABRE. *Mol. Phys.* **2019**, *117* (19), 2762−2771.

(19) Svyatova, A.; Skovpin, I. V.; Chukanov, N. V.; Kovtunov, K. V.; Chekmenev, E. Y.; Pravdivtsev, A. N.; Hövener, J.; Koptyug, I. V. 15N MRI of SLIC-SABRE Hyperpolarized 15N-Labelled Pyridine and Nicotinamide. *Chem. Eur. J.* **2019**, *25* (36), 8465−8470.

(20) Dücker, E. B.; Kuhn, L. T.; Münnemann, K.; Griesinger, C. Similarity of SABRE Field Dependence in Chemically Different Substrates. *J. Magn. Reson.* **2012**, *214*, 159−165.

(21) Adams, R. W.; Duckett, S. B.; Green, R. A.; Williamson, D. C.; Green, G. G. R. A Theoretical Basis for Spontaneous Polarization Transfer in Non-Hydrogenative Para Hydrogen-Induced Polarization. *J. Chem. Phys.* **2009**, *131* (19), 194505.

(22) Pravdivtsev, A. N.; Yurkovskaya, A. V.; Vieth, H.; Ivanov, K. L.; Kaptein, R. Level Anti-Crossings Are a Key Factor for Understanding Para-Hydrogen-Induced Hyperpolarization in SABRE Experiments. *ChemPhysChem* **2013**, *14* (14), 3327−3331.

(23) Barskiy, D. A.; Knecht, S.; Yurkovskaya, A. V.; Ivanov, K. L. SABRE: Chemical Kinetics and Spin Dynamics of the Formation of Hyperpolarization. *Prog. Nucl. Magn. Reson. Spec.* **2019**, *114*−*115*, 33−70.

(24) Schmidt, A. B.; Bowers, C. R.; Buckenmaier, K.; Chekmenev, E. Y.; de Maissin, H.; Eills, J.; Ellermann, F.; Glöggler, S.; Gordon, J. W.; Knecht, S.; Koptyug, I. V.; Kuhn, J.; Pravdivtsev, A. N.; Reineri, F.; Theis, T.; Them, K.; Hövener, J.-B. Instrumentation for Hydrogenative Parahydrogen-Based Hyperpolarization Techniques. *Anal. Chem.* **2022**, *94* (1), 479−502.
(25) Shchepin, R. V.; Barskiy, D. A.; Coffey, A. M.; Theis, T.; Shi, F.; Warren, W. S.; Goodson, B. M.; Chekmenev, E. Y. 15N Hyperpolarization of Imidazole-15N2 for Magnetic Resonance PH Sensing via SABRE-SHEATH. *ACS Sens.* **2016**, *1* (6), 640−644.
(26) Theis, T.; Ortiz, G. X.; Logan, A. W. J.; Claytor, K. E.; Feng, Y.; Huhn, W. P.; Blum, V.; Malcolmson, S. J.; Chekmenev, E. Y.; Wang, Q.; et al. Direct and Cost-Efficient Hyperpolarization of Long-Lived Nuclear Spin States on Universal 15N2-Diazirine Molecular Tags. *Sci. Adv.* **2016**, *2* (3), No. e1501438.
(27) Rayner, P. J.; Burns, M. J.; Olaru, A. M.; Norcott, P.; Fekete, M.; Green, G. G. R.; Highton, L. A. R.; Mewis, R. E.; Duckett, S. B. Delivering Strong 1H Nuclear Hyperpolarization Levels and Long Magnetic Lifetimes through Signal Amplification by Reversible Exchange. *Proc. Natl. Acad. Sci. U. S. A.* **2017**, *114* (16), E3188−E3194.
(28) Iali, W.; Rayner, P. J.; Alshehri, A.; Holmes, A. J.; Ruddlesden, A. J.; Duckett, S. B. Direct and Indirect Hyperpolarisation of Amines Using Para Hydrogen. *Chem. Sci.* **2018**, *9*, 3677−3684.
(29) Mewis, R. E.; Green, R. A.; Cockett, M. C. R.; Cowley, M. J.; Duckett, S. B.; Green, G. G. R.; John, R. O.; Rayner, P. J.; Williamson, D. C. Strategies for the Hyperpolarization of Acetonitrile and Related Ligands by SABRE. *J. Phys. Chem. B* **2015**, *119* (4), 1416−1424.
(30) Kim, S.; Min, S.; Chae, H.; Jeong, H. J.; Namgoong, S. K.; Oh, S.; Jeong, K. Hyperpolarization of Nitrile Compounds Using Signal Amplification by Reversible Exchange. *Molecules* **2020**, *25* (15), 3347.
(31) Shchepin, R. V.; Barskiy, D. A.; Coffey, A. M.; Goodson, B. M.; Chekmenev, E. Y. NMR Signal Amplification by Reversible Exchange of Sulfur-Heterocyclic Compounds Found in Petroleum. *ChemistrySelect* **2016**, *1* (10), 2552.
(32) Iali, W.; Roy, S. S.; Tickner, B. J.; Ahwal, F.; Kennerley, A. J.; Duckett, S. B. Hyperpolarising Pyruvate through Signal Amplification by Reversible Exchange (SABRE). *Angew. Chem.* **2019**, *131* (30), 10377−10381.
(33) Tickner, B. J.; Ahwal, F.; Whitwood, A. C.; Duckett, S. B. Reversible Hyperpolarization of Ketoisocaproate Using Sulfoxide-containing Polarization Transfer Catalysts. *ChemPhysChem* **2021**, *22* (1), 13−17.
(34) Iali, W.; Rayner, P. J.; Duckett, S. B. Using Parahydrogen to Hyperpolarize Amines, Amides, Carboxylic Acids, Alcohols, Phosphates, and Carbonates. *Sci. Adv.* **2018**, *4* (1), No. eaao6250.
(35) Vaneeckhaute, E.; De Ridder, S.; Tyburn, J.; Kempf, J. G.; Taulelle, F.; Martens, J. A.; Breynaert, E. Long-Term Generation of Longitudinal Spin Order Controlled by Ammonia Ligation Enables Rapid SABRE Hyperpolarized 2D NMR. *ChemPhysChem* **2021**, *22* (12), 1150.
(36) Rayner, P. J.; Tickner, B. J.; Iali, W.; Fekete, M.; Robinson, A. D.; Duckett, S. B. Relayed Hyperpolarization from Para-Hydrogen Improves the NMR Detectability of Alcohols. *Chem. Sci.* **2019**, *10* (33), 7709−7717.
(37) Richardson, P. M.; Iali, W.; Roy, S. S.; Rayner, P. J.; Halse, M. E.; Duckett, S. B. Rapid 13C NMR Hyperpolarization Delivered from Para-Hydrogen Enables the Low Concentration Detection and Quantification of Sugars. *Chem. Sci.* **2019**, *10* (45), 10607−10619.
(38) Rayner, P. J.; Richardson, P. M.; Duckett, S. B. The Detection and Reactivity of Silanols and Silanes Using Hyperpolarized 29Si Nuclear Magnetic Resonance. *Angew. Chem.* **2020**, *132* (7), 2732−2736.
(39) Vaneeckhaute, E.; Tyburn, J.-M.; Kilgour, D.; Kempf, J. G.; Taulelle, F.; Martens, J. A.; Breynaert, E. Hyperpolarised Magnetic Resonance of Exchangeable Protons Using Parahydrogen and Aminosilane. *J. Phys. Chem. C* **2020**, *124* (27), 14541−14549.
(40) Štěpánek, P.; Sanchez-Perez, C.; Telkki, V.-V.; Zhivonitko, V. V.; Kantola, A. M. High-Throughput Continuous-Flow System for SABRE Hyperpolarization. *J. Magn. Reson.* **2019**, *300*, 8−17.
(41) Lehmkuhl, S.; Wiese, M.; Schubert, L.; Held, M.; Küppers, M.; Wessling, M.; Blümich, B. Continuous Hyperpolarization with Parahydrogen in a Membrane Reactor. *J. Magn. Reson.* **2018**, *291*, 8−13.
(42) Cavallari, E.; Carrera, C.; Boi, T.; Aime, S.; Reineri, F. Effects of Magnetic Field Cycle on the Polarization Transfer from Parahydrogen to Heteronuclei through Long-Range J-Couplings. *J. Phys. Chem. B* **2015**, *119* (31), 10035−10041.
(43) Stewart, N. J.; Kumeta, H.; Tomohiro, M.; Hashimoto, T.; Hatae, N.; Matsumoto, S. Long-Range Heteronuclear J-Coupling Constants in Esters: Implications for 13C Metabolic MRI by Side-Arm Parahydrogen-Induced Polarization. *J. Magn. Reson.* **2018**, *296*, 85−92.
(44) Knecht, S.; Barskiy, D. A.; Buntkowsky, G.; Ivanov, K. L. Theoretical Description of Hyperpolarization Formation in the SABRE-Relay Method. *J. Chem. Phys.* **2020**, *153* (16), 164106.
(45) Tickner, B. J.; Rayner, P. J.; Duckett, S. B. Using SABRE Hyperpolarized 13C NMR to Interrogate Organic Transformations of Pyruvate. *Anal. Chem.* **2020**, *92* (13), 9095−9103.
(46) Chae, H.; Min, S.; Jeong, H. J.; Namgoong, S. K.; Oh, S.; Kim, K.; Jeong, K. Organic Reaction Monitoring of a Glycine Derivative Using Signal Amplification by Reversible Exchange-Hyperpolarized Benchtop Nuclear Magnetic Resonance Spectroscopy. *Anal. Chem.* **2020**, *92* (16), 10902−10907.
(47) Keshari, K. R.; Wilson, D. M. Chemistry and Biochemistry of 13C Hyperpolarized Magnetic Resonance Using Dynamic Nuclear Polarization. *Chem. Soc. Rev.* **2014**, *43* (5), 1627−1659.
(48) Kennedy, B. W. C.; Kettunen, M. I.; Hu, D.-E.; Brindle, K. M. Probing Lactate Dehydrogenase Activity in Tumors by Measuring Hydrogen/Deuterium Exchange in Hyperpolarized l-[1−13C, U-2H] Lactate. *J. Am. Chem. Soc.* **2012**, *134* (10), 4969−4977.
(49) Duckett, S. B.; Newell, C. L.; Eisenberg, R. More than INEPT: Parahydrogen and INEPT+ Give Unprecedented Resonance Enhancement to Carbon-13 by Direct Proton Polarization Transfer. *J. Am. Chem. Soc.* **1993**, *115* (3), 1156−1157.
(50) Kozinenko, V. P.; Kiryutin, A. S.; Yurkovskaya, A. V.; Ivanov, K. L. Polarization of Low-γ Nuclei by Transferring Spin Order of Parahydrogen at High Magnetic Fields. *J. Magn. Reson.* **2019**, *309*, 106594.
(51) Haake, M.; Natterer, J.; Bargon, J. Efficient NMR Pulse Sequences to Transfer the Parahydrogen-Induced Polarization to Hetero Nuclei. *J. Am. Chem. Soc.* **1996**, *118* (36), 8688−8691.
(52) Svyatova, A.; Kozinenko, V. P.; Chukanov, N. V.; Burueva, D. B.; Chekmenev, E. Y.; Chen, Y.-W.; Hwang, D. W.; Kovtunov, K. V.; Koptyug, I. V. PHIP Hyperpolarized [1−13C] Pyruvate and [1−13C] Acetate Esters via PH-INEPT Polarization Transfer Monitored by 13C NMR and MRI. *Sci. Rep.* **2021**, *11* (1), 5646.
(53) Eshuis, N.; Aspers, R. L. E. G.; van Weerdenburg, B. J. A.; Feiters, M. C.; Rutjes, F. P. J. T.; Wijmenga, S. S.; Tessari, M. Determination of Long-Range Scalar 1H-1H Coupling Constants Responsible for Polarization Transfer in SABRE. *J. Magn. Reson.* **2016**, *265*, 59−66.
(54) Eisenschmid, T. C.; McDonald, J.; Eisenberg, R.; Lawler, R. G. INEPT in a Chemical Way. Polarization Transfer from Para Hydrogen to Phosphorus-31 by Oxidative Addition and Dipolar Relaxation. *J. Am. Chem. Soc.* **1989**, *111* (18), 7267−7269.
(55) Knecht, S.; Kiryutin, A. S.; Yurkovskaya, A. V.; Ivanov, K. L. Re-Polarization of Nuclear Spins Using Selective SABRE-INEPT. *J. Magn. Reson.* **2018**, *287*, 10−14.

https://doi.org/10.1021/acs.jpclett.2c01442
J. Phys. Chem. Lett. 2022, 13, 6859−6866